AIAA JOURNAL
Vol. 41, No. 2, February 2003

Technical Notes

TECHNICAL NOTES are short manuscripts describing new developments or important results of a preliminary nature. These Notes cannot exceed six manuscript pages and three figures; a page of text may be substituted for a figure and vice versa. After informal review by the editors, they may be published within a few months of the date of receipt. Style requirements are the same as for regular contributions (see inside back cover).

Extrapolation Effects on Coupled Computational Fluid Dynamics/ Computational Structural Dynamics Simulations

G. S. L. Goura,* K. J. Badcock,† M. A. Woodgate,‡ and B. E. Richards§
University of Glasgow, Glasgow, Scotland G12 8QQ, United Kingdom

I. Introduction

HISTORICALLY, intergrid transformation methods have been developed for wing aeroelastic simulations based on panel aerodynamic models. Here, the fluid and structural surfaces are both defined on a plate. In contrast, flow solvers based on the Navier–Stokes equations require a description of the full aerodynamic shape. However, wing structural models are often still simplified, for example, to a plate or box. Further background on intergrid transformations for fluid-structure interaction can be found in Refs. 1 and 2.

To deal with cases of nonmatching surfaces, transformation methods typically project the aerodynamic surface grid points onto the structural surface, or possibly project the aerodynamic and structural points onto a neutral surface. The displacements of the projected points are calculated using the spline methods originally designed for linear aerodynamics. The aerodynamic positions are then deduced by supposing that each aerodynamic point is attached to its projection by a rigid arm. This latter assumption leads to shape distortion when rigid motions are applied.[3] Another method, called constant volume tetrahedra was proposed in Ref. 4. These references, and several others, have primarily focused on the treatment of the displacement out of the plane of the structural model.

A second problem arises when the planform of the structural and fluid models is not the same, as happens for example when a wing box model is used to treat the structure. The in-plane component of displacement must then be extrapolated beyond the bounds of the structural model. The performance of two methods commonly used for this extrapolation, and the influence of these on the aeroelastic response observed, is the subject of this Note.

II. Formulation

The formulation for the aeroelastic code is given in Ref. 5. The flow solver is a parallel multiblock code whose features have been documented in Ref. 6. In the current work it is used in Euler mode. The structural model is in the form of modes derived from a finite element model. The two solutions are coupled in time by iterating between them, passing loads from the flow code to the structural code, and displacements back the other way. For unsteady problems the sequencing is done within the pseudotime loop used for the flow solver and removes sequencing errors. The mesh movement for the aerodynamic solver is done using transfinite interpolation of displacements.[7]

We restrict ourselves in this Note to the case of a wing modeled structurally by a plate. This case is interesting as a building block to more complex structural descriptions. Transformation of data between the two grids is broken into two components in and out of the plane of the structural model. The outplane treatment follows the considerations of Ref. 5. The in-plane treatment turns out to have a much stronger influence on the test case considered next. The two approaches used are the infinite plate spline (IPS)[8] and linear interpolation. For IPS a solution of the thin-plate equation is forced to pass through the known structural points and is then evaluated at the projected aerodynamic points for the required displacements. For linear interpolation each projected fluid point is associated with a triangle on the structural mesh, and the deformation is calculated using a linear approximation within the triangle. In both cases the relationship between displacements on the fluid and structural grids is linear, and the principle of virtual work is then applied for transferring forces.

III. Test Cases

The target application for this work was the aeroelastic response of the multidisciplinary optimization (MDO) wing in the transonic range.[9] The wing has a span of 36 m, and the planform is shown in Fig. 1. The profile is a thick supercritical section. The extent of the structural model is indicated in the dark shaded region. The planform of the fluid and structural models do not match, and the in-plane components of the displacements have to be extrapolated beyond the limits of the structural grid. The structural model consists of 18 modes between 0.88 and 14.97 Hz. Static and dynamic results are presented for a case with freestream Mach number 0.88 and an altitude of 2 km. The angle of attack is found so that the deformed wing has a lift coefficient of 0.1686 based on the wing surface area.

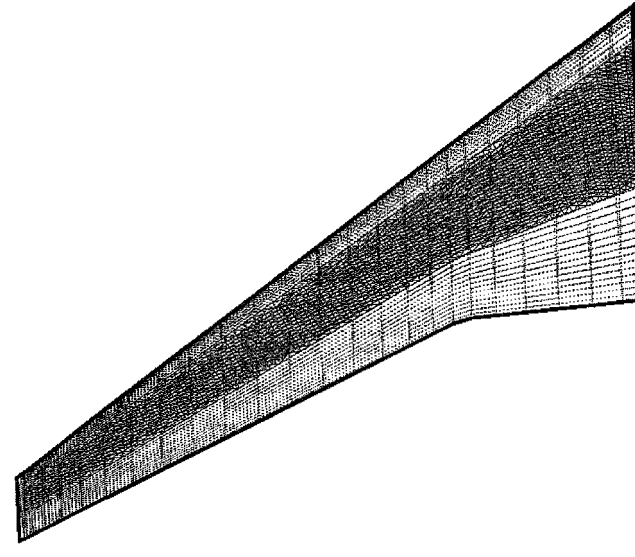

Fig. 1 MDO wing planform. The dark shaded region indicates the extent of the structural model.

Received 19 November 2001; revision received 4 August 2002; accepted for publication 19 September 2002.

*Research Student, Department of Aerospace Engineering.
†Senior Lecturer, Department of Aerospace Engineering. Member AIAA.
‡Research Assistant, Department of Aerospace Engineering.
§Professor, Department of Aerospace Engineering. Associate Fellow AIAA.

For the dynamic calculation the wing is given an initial velocity in the first mode, and the resulting evolution, which indicates flutter, is then calculated.

IV. Results

We first examine how the mode shapes are transformed onto the fluid grid from applied motions in single modes on the structural grid. To gain an idea of the effect of the reduced structural planform a second wing, the AGARD 445.6 wing[10] was first considered. A full planform plate structural model was available for this wing. Tests were conducted on the full model and also on a cutdown plate, which had the leading- and trailing-edge portions removed to reproduce the problem encountered for the MDO wing.

The transformed mode shapes are presented as the profile at 75% of the span. When a deflection is applied to the first torsion mode and the full structural model is used for the transformation, the IPS and linear methods give identical results. However, when the reduced plate model is used the transformed profile on the aerodynamic grid obtained using IPS has a camber in the extrapolated regions, which is introduced by the far-field behavior of IPS, as shown at the leading edge in Fig. 2. In contrast the linear profile agrees well with the full plate model. This effect has previously been noted in Ref. 11. Similar differences can be observed between the transformed torsion mode shapes using the IPS and linear methods for the MDO wing case.

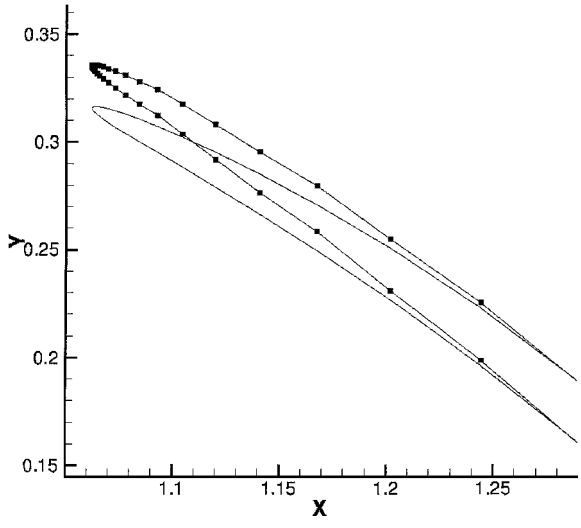

Fig. 2 Transformed torsion mode shape in the leading-edge region for AGARD 445.6 wing at 75% span using the full and reduced plate model. The profile marked with the squares is obtained using IPS and linear for the full plate model. The profile indicated by the line only is obtained using IPS on the reduced plate grid.

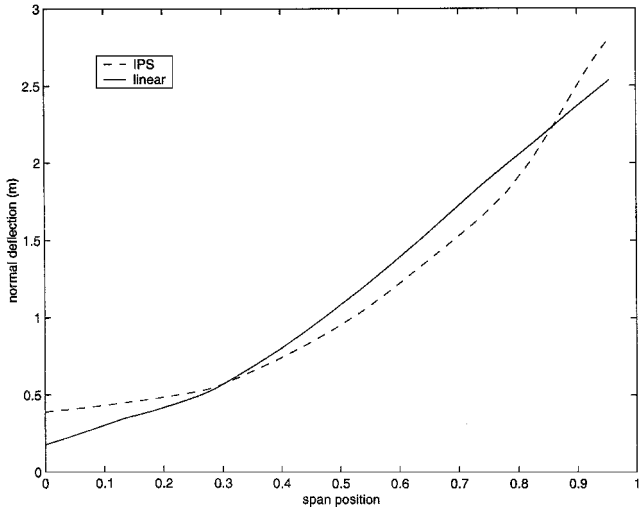

Fig. 3 Aerostatic comparisons for MDO case 3 for trimmed conditions using linear and IPS transformations. The span position is measured from 0 at the root to 1 at the tip, and the normal deflection plotted is that at the trailing edge. Here the Mach number is 0.88, the altitude is 2 km, and the incidence is 0.3743 deg for the linear method and −0.135 deg for IPS (both resulting in a lift coefficient of 0.1686).

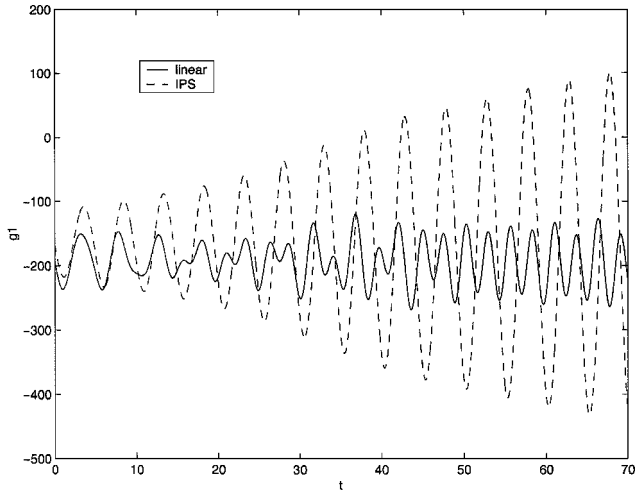

Fig. 4 Comparison of modal time histories for MDO dynamic case using linear and IPS transformations. Here the Mach number is 0.88, the altitude is 2 km, and the incidence is 0.3743 deg for the linear method and −0.135 deg for IPS (both resulting in an initial lift coefficient of 0.1686).

The aerostatic deflection for the MDO test case along the trailing edge is shown in Fig. 3. The additional camber introduced by the IPS extrapolation results in a larger wing deflection at the tip than when the linear method is used. The time history for the first mode for the dynamic calculation is shown in Fig. 4 and shows that the IPS result has a much more vigorous response. The only difference in the details of these simulations was the in-plane transformation treatment, that is, all grids, models, and numerical parameters were identical otherwise.

V. Conclusions

These results have shown that the simulation of aeroelastic responses of simple wing geometries can be strongly influenced by the transformation method used to couple the fluid and structural grids when the planforms do not match. Inspection of the geometrical effect of the extrapolation for the aerodynamic profile shows that IPS introduces an unwanted camber and that linear extrapolation preserves the mode shape well. The effect of the distorted profile using IPS is to increase the aerostatic and dynamic responses of the wing. It is concluded that for similar cases the geometrical influence of the in-plane treatment should be inspected visually before coupled calculations are attempted.

Acknowledgments

The authors are grateful to Anders Karlsson of SAAB and Michael Henshaw of BAE Systems for their assistance with the MDO test case and their general comments on this work.

References

[1]Smith, M. J., Hodges, D. H., and Cesnik, C. E. S., "Evaluation of Computational Algorithms Suitable for Fluid-Structure Interactions," *Journal of Aircraft*, Vol. 37, No. 2, 2000, pp. 282–294.

[2]Smith, M. J., Cesnik, C. E. S., Hodges, D. H., and Moran, K. J., "Evaluation of Some Data Transfer Algorithms for Noncontiguous Meshes," *Journal of Aerospace Engineering*, Vol. 13, No. 2, 2000, pp. 52–58.

[3]Chen, P. C., and Jadic, I., "Interfacing of Fluid and Structural Models via Innovative Boundary Element Method," *AIAA Journal*, Vol. 36, No. 2, 1998, pp. 282–287.

[4]Goura, G. S. L., Badcock, K. J., Woodgate, M. A., and Richards, B. E., "A Data Exchange Method for Fluid-Structure Interaction Problems," *Aeronautical Journal*, Vol. 105, No. 1046, 2001, pp. 215–221.

[5]Goura, G. S. L., Badcock, K. J., Woodgate, M. A., and Richards, B. E., "Implicit Method for the Time Marching Analysis of Flutter," *Aeronautical Journal*, Vol. 105, No. 1046, 2001, pp. 199–214.

[6]Badcock, K. J., Richards, B. E., and Woodgate, M. A., "Elements of Computational Fluid Dynamics on Block Structured Grids Using Implicit

Flow Solvers," *Progress in Aerospace Sciences*, Vol. 36, No. 5–6, 2000, pp. 351–392.

[7]Dubuc, L., Cantariti, F., Woodgate, M., Gribben, B., Badcock, K. J., and Richards, B. E., "Solution of the Euler Unsteady Equations Using Deforming Grids," *AIAA Journal*, Vol. 36, No. 8, 1998, pp. 1417–1424.

[8]Harder, R. L., and Desmarais, R. N., "Interpolation Using Surface Splines," *Journal of Aircraft*, Vol. 9, No. 2, 1972, pp. 189–191.

[9]Girodroux-Lavigne, P., Grisval, J. P., Guillemot, S., Henshaw, M., Karlsson, A., Selmin, V., Smith, J., Teupootahiti, E., and Winzell, B., "Comparative Study of Advanced Fluid-Structure Interaction Methods in the Case of a Highly Flexible Wing (Results from the UNSI Program)," International Forum Aeroelasticity Structural Dynamics, Confereration of European Aerospace Societies/AIAA/Asociancion Espanola de Ingenieros Aeronauticos, June 2001.

[10]Yates, E. C., "AGARD Standard Aeroelastic Configurations for Dynamic Response I: Wing 445.6," Rept. 765, AGARD, 1988.

[11]Brown, S. A., "Displacement Extrapolation for CFD and CSM Analysis," AIAA Paper 97-1090, April 1997.

E. Livne
Associate Editor

Vortex Interaction of a Delta-Wing Flowfield

C. Shih* and Z. Ding†
Florida A&M University and Florida State University, Tallahassee, Florida 32310

Introduction

FOR the past several decades aspects of flows over delta wings, especially phenomena associated with leading-edge vortices, have been studied extensively.[1–7] At moderate angles of attack, the delta-wing flowfield is dominated by the presence of a pair of well-organized leading-edge vortices, commonly known as the primary vortices. Underneath the primary vortex the outboard-moving boundary layer separates as it approaches the leading edge to form a counter-rotating secondary vortex. Based on the averaged flow measurements, the secondary vortex is relatively small in size and peak magnitude as compared to the primary vortex. Additionally, its close proximity to the surface and the leading-edge shear layer makes it hard to be measured or computed accurately. These factors frequently lead to the conclusion that the secondary vortex only plays a secondary role and can be neglected in the delta-wing analysis. This characterization, however, has been challenged recently because it has been shown both experimentally[8,9] and numerically[10,11] that the interaction between the primary and the secondary vortices can be important in consideration of the overall flow behavior. The present experimental study examines in detail this interaction and its contribution to the unsteady characteristics of the entire flowfield. In this work we carried out experiments using particle image velocimetry (PIV) to study the leading-edge vortex flow over a delta wing. Our main objective is to explore the role played by the secondary vortex including its interaction with the primary vortex and its influence on the global vortex dynamics of the flowfield.

Experimental Setup

The experiments were carried out in a water towing tank facility. The delta wing has a leading-edge sweep angle of 60 deg and a root chord length of 13.0 cm. The experimental Reynolds number, based on the root chord length and the towing velocity, was 9.8×10^3. Both sides of the leading edge are sharp and beveled 45 deg leeward. The delta wing was set at an angle of attack of 12.5 deg. Detailed description of the experiment can be found in a previous paper.[8] The focus of the current study was on the detailed characterization of the unsteady motions of the leading-edge vortex flowfield using PIV technique. An 18-W argon-ion laser beam was expanded into pulsed laser sheets using a 24-faceted rotating mirror for image illumination. Tracer particles used were 10-μm silver-coated hollow glass beads with a specific gravity of 1.3. The PIV images were digitized by an optical scanner from 35-mm film images. The maximum error of the PIV technique in acquiring the instantaneous velocity and vorticity data was estimated to be 1 and 5%, respectively. More detailed discussions of the PIV technique can be found in the literature.[12,13]

Results and Discussion

To gain quantitative understanding of the behavior of the leading-edge vortex system, PIV measurements are taken along several crossflow planes that are normal to the freestream. Located on these planes, the y and z coordinates are defined, respectively, as the cross-stream and the span-wise directions, with their origin fixed at the left-side leading edge (as viewed from the trailing edge). In the discussions that follow, solid lines in the vorticity contour plots denote positive (clockwise) vorticity, whereas dashed lines denote negative (counterclockwise) vorticity. A time-averaged vorticity plot at a representative crossflow plane (50% chord, $x/C = 0.5$) is shown in Fig. 1. It can be seen that the primary vortex (solid lines) is well defined with a coherent vortex core. Located close to the leading edge and directly underneath the primary vortex, there exists the counter-rotating secondary vortex (dashed lines), which has a smaller amplitude as compared with the primary vortex. A strong shear layer emerges further outboard at the leading edge; high-amplitude vortical eddies can be observed to appear along the shear layer.

Figure 2 shows a representative sequence of the instantaneous primary/secondary vortex interaction at $x/C = 0.5$. The first frame is taken to be the reference time $t^+ = tU_\infty/C = 0.0$ (Fig. 2a) when the elongated primary vortex is tightly connected to the separating shear layer, allowing a continuous feeding of the shear layer vorticity into the primary vortex. During the next two instants (Figs. 2b and 2c), several individualized vortical eddies inside the primary vortex appear to roll up and coalesce into a highly concentrated vortical structure. Moreover, the secondary vortex is lifted upward to penetrate into the separating shear layer to sever the linkage between the primary vortex and the shear layer. In Fig. 2d, $t^+ = 0.384$, the shear layer appears to reconnect back to the primary vortex, and its primary vortical structure bears a close resemblance to the vortical structure in Fig. 2a, indicating the completion of a full interaction cycle. Through the analysis of a sequence of instantaneous PIV vorticity fields, it is observed that the interaction process indeed repeats itself in a quasi-periodic manner. Careful investigation of the interaction sequence reveals that each cycle consists of the following four repetitive stages: primary vortex induction/secondary vortex ejection, effect of the ejection process on the primary vortex, weakening of both the primary and secondary vortices, and reconnection of the primary vortex and the shear layer.

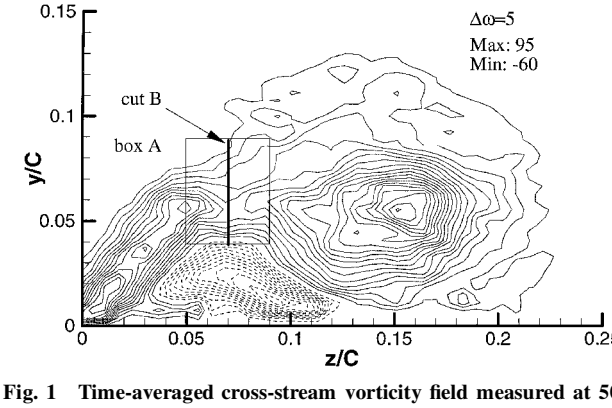

Fig. 1 Time-averaged cross-stream vorticity field measured at 50% chord.

Received 11 July 2000; revision received 10 September 2002; accepted for publication 19 September 2002.

*Professor, Department of Mechanical Engineering. Associate Fellow AIAA.

†Graduate Research Assistant, Department of Mechanical Engineering; currently Research Scientist, Exxon Mobil Upstream Research Company, Houston, TX 77252.